Published in final edited form as:
Virology. 2011 January 20; 409(2): 319–327. doi:10.1016/j.virol.2010.10.030.

The host outer membrane proteins OmpA and OmpC are associated with the *Shigella* phage Sf6 virion

Haiyan Zhao[‡], **Reuben D. Sequeira**[‡], **Nadezhda A. Galeva**[†], and **Liang Tang**[‡,*]

Haiyan Zhao: zhaohy@ku.edu; Reuben D. Sequeira: sequen@ku.edu; Nadezhda A. Galeva: galeva@ku.edu

[‡] Department of Molecular Biosciences, University of Kansas, 1200 Sunnyside Avenue, Lawrence, KS 66045

[†] Analytical Proteomics Laboratory, Structural Biology Center, University of Kansas, 2034 Becker Drive, Lawrence, KS 66047

Abstract

Assembly of dsDNA bacteriophage is a precisely programmed process. Potential roles of host cell components in phage assembly haven't been well understood. It was previously reported that two unidentified proteins were present in bacteriophage Sf6 virion (Casjens et al, 2004, J. Mol. Biol. 339, 379–394, Figure 2A). Using tandem mass spectrometry, we have identified the two proteins as outer membrane proteins (OMPs) OmpA and OmpC from its host Shigella flexneri. The transmission electron cryo-microscopy structure of Sf6 shows significant density at specific sites at the phage capsid inner surface. These density fit well with the characteristic beta-barrel domains of OMPs, thus may be due to the two host proteins. Locations of these density suggest a role in Sf6 morphogenesis reminiscent of phage-encoded cementing proteins. These data indicate a new, OMP-related phage:host linkage, adding to previous knowledge that some lambdoid bacteriophage genomes contain OmpC-like genes that express phage-encoded porins in the lysogenic state.

Keywords

virus assembly; bacteriophage; cementing protein; Shigella; outer membrane protein; OmpA; OmpC

INTRODUCTION

Assembly of large, complex viruses involves hundreds of viral structural proteins as well as the viral nucleic acid that undergo programmed molecular interactions and structural transitions along the assembly cascade. In many tailed double-stranded DNA (dsDNA) bacteriophage, assembly of progeny phage begins with formation of a proteinaceous capsid precursor termed procapsid, which is made up of numerous viral proteins including the capsid protein, the portal protein, the pilot protein and the scaffolding protein. This is followed by packaging of viral DNA into the procapsid, maturation of the metastable procapsid into the stable capsid, and attachment of additional viral structural components

[*]Correspondence author: L.T. Department of Molecular Biosciences, University of Kansas, 1200 Sunnyside Avenue, Lawrence, KS 66045, Tel: 785-864-5838, Fax: 785-864-5294, tangl@ku.edu.

(Steven et al., 2005). A characteristic in the transition from the procapsid to the mature capsid is massive structural rearrangements involving local conformational changes and large-scale rotational and translational movements of capsid protein subunits (Gertsman et al., 2009; Johnson, 2010; Wikoff et al., 2000), which is accompanied by insertion of phage DNA and expelling of the scaffolding protein (Dokland, 1999; Fane and Prevelige, 2003; Rao and Feiss, 2008). Additional phage-encoded cementing proteins bind to the exterior of the matured capsid to increase the capsid stability in some cases such as T4 (Fokine et al., 2004), lambda (Yang et al., 2000), L (Tang et al., 2006), phi29 (Morais et al., 2005), BPP-1 (Dai et al., 2010) and epsilon15 (Jiang et al., 2008). These features in dsDNA bacteriophage assembly are shared by herpesviruses (Homa and Brown, 1997; Johnson, 2010; Steven et al., 2005; Trus et al., 1996).

Phage assembly has been viewed and studied primarily as an outcome of molecular interactions of viral proteins. Structural studies of purified phage capsid, procapsid and structural proteins in vitro have offered rich insights into molecular mechanisms of various steps of phage assembly (Gertsman et al., 2009; Johnson, 2010; Steven et al., 2005). However, virus assembly occurs in host cells, where crowdedness of cellular contents provides abundant chances of intermolecular interactions between host and viral proteins. It hasn't been well understood if and how components of host cells play potential structural roles in phage assembly. Examples of host factors involved in phage assembly have been documented, for instance, the *E. coli* integration host factor that helps bend phage lambda DNA for terminase-DNA interaction prior to DNA packaging (de Beer et al., 2002; Xin and Feiss, 1993), and the host chaperone GroEL that interacts with a phage-encoded, GroES-like protein gp31 in phage T4 and aids phage protein folding (Clare et al., 2009; van der Vies, Gatenby, and Georgopoulos, 1994). However, these host proteins are not structurally involved in phage assembly and/or are not present in assembled phage virion. Enveloped viruses can derive host proteins through acquisition of host membrane, which does not generally involve specific interactions between viral and host proteins. Proteins of cellular origin were identified in herpesvirus virion by proteomic approaches (Bechtel, Winant, and Ganem, 2005; Loret, Guay, and Lippe, 2008; Zhu et al., 2005). Nevertheless, it is unclear if any of these proteins plays an active biological role in herpesvirus lifecycles. The presence of these host proteins in the virion may be merely a consequence of their abundance in host cytoplasm, and no specific interactions between these host proteins and viral structural proteins have been reported. Examples of eukaryotic viruses incorporating specific host proteins in virions include papovavirus whose genomic DNA is associated with host-derived histones (Fanning and Zhao, 2009), and human immunodeficiency virus which packs host-encoded cyclophilin A (Franke, Yuan, and Luban, 1994). The roles of these host proteins in virus morphogenesis haven't been studied in detail.

Sf6 belongs to the *Podoviridae* family of tailed dsDNA bacteriophage (Casjens et al., 2004; Gemski, Koeltzow, and Formal, 1975). Sf6 infects *Shigella flexneri*, an important human pathogen that can cause acute diarrhea and bacillary dysentery. Sf6 is capable of changing host lipopolysaccharide structure using a horizontal gene transfer mechanism, therefore altering the serotype and virulence of the host (Lindberg et al., 1978). Previous work showed that all structural proteins of Sf6 including the capsid protein, the portal, the injection proteins and the tail proteins are largely homologous to those of well-studied, closely related phage P22, with about the same protein sizes and the same amounts in virions (Casjens et al., 2004). Interestingly, two unidentified, potentially non-virally encoded, proteins were found in the Sf6 virion but not in P22 (Casjens et al., 2004). Here we report identification of these two proteins as outer membrane proteins (OMPs), OmpA and OmpC, from the host Shigella flexneri using tandem mass spectrometry. The transmission electron cryo-microscopy (cryoTEM) structure of Sf6 shows significant density at specific sites at the phage capsid inner surface, which is not present in phage P22. This and further docking

analysis provide evidence that these density may be due to the two host proteins. Thus, the two host proteins are likely associated with the Sf6 virion at the inner capsid surface. These density are located at sites that bridge adjacent capsid protein subunits, suggesting that the two host proteins may be involved in Sf6 morphogenesis in a manner reminiscent of phage-encoded cementing proteins that confer capsid stability. Implication of association of the two OMPs with Sf6 on the OMP folding pathway and potential spatial coupling of phage assembly and the host protein folding machinery is also discussed. It was previously reported that genomes of a few lambdoid bacteriophage contain OmpC-like genes that were expressed during the lysogenic state, and these phage used the host OmpC as their cellular receptor (Blasband, Marcotte, and Schnaitman, 1986; Highton et al., 1985). Thus, our finding suggests a new phage:host linkage, in which OMPs may play a structural role in phage assembly.

RESULTS

Identification of OmpA and OmpC in the Sf6 virion

The Sf6 virions were purified to homogeneity with CsCl step gradient ultracentrifugation. The gradient was set up such that it contained 2ml 20% sucrose solution on the top, 2ml 1.4g/ml CsCl solution in the middle, and 2ml 1.6g/ml CsCl solution at the bottom. As bacterial debris has a density in the range of 1.15–1.25 g/ml (Ishidate et al., 1986), membranous fragments and other debris from lysed bacteria migrated within the sucrose gradient but didn't penetrate into the 1.4 g/ml CsCl gradient. The Sf6 virions formed a sharp opalescent band at the boundary between the 1.4 and 1.6 g/ml CsCl solutions. A consecutive run of CsCl gradient ultracentrifugation was conducted to thoroughly remove residual contaminants. Negative staining electron microscopy of the purified Sf6 virions demonstrated the high homogeneity of the preparation (Figure 1A). The Sf6 virion showed an angular, icosahedral capsid and a short tail emanating from a single 5-fold vertex (Figure 1A), reminiscent of bacteriophage P22 (Jiang et al., 2003; Tang et al., 2006). This confirms that the purified Sf6 was mature virions but not procapsids. SDS polyacrylamide gel electrophoresis (PAGE) of the purified Sf6 virion showed two bands corresponding to the two unidentified proteins that are not present in phage P22 as previously reported (Casjens et al., 2004) (Figure 1B). The molecular mass of these two proteins are in the range of 34 to 42 kDa, and can not be explained by virally encoded proteins based on analysis of open reading frames in the Sf6 genome sequence (Casjens et al., 2004). The scaffolding protein of Sf6 contains 294 residues with a molecular weight of 33,486Da, but may not be the candidate for any of these two protein bands, as scaffolding proteins are expelled from phage capsid during DNA packaging and maturation and are generally not present in mature virions. To identify the two proteins, the two bands were excised and subjected to in-gel tryptic digestion followed by tandem mass spectrometry. Mascot (Matrix Science) and X! Tandem (www.thegpm.org) algorithms were used to perform MS/MS database search. The Scaffold software (Proteome Software Inc.) was used to combine and validate MS/MS based peptide and protein identifications. The analysis unambiguously identified the two proteins as the outer membrane proteins OmpA and OmpC from the *Shigella* host, respectively (Table 1). A total of 12 and 14 distinct peptides were identified for OmpA and OmpC, with sequence coverage of 47% and 52% respectively (Tables 1 and 2). It is known that OmpA and OmpC both contain an N-terminal signal peptide that is cleaved upon translocation across the bacterial inner membrane (Bernstein, 2000; Holland, 2004; von Heijne, 1990). The mass spectrometry data did not address whether their N-terminal signal peptides were cleaved. We performed N-terminal sequencing for the two bands excised from the SDS gel. The results showed an N-terminal sequence of "APKDN" and "AEVYN" respectively, matching residues 22–26 in the full-length OmpA and OmpC sequences. This indicates that the signal peptides were cleaved from the two host proteins. The positions of cleavage are

consistent with those predicted with the SignalP server (Bendtsen et al., 2004), and residues 1–21 in both proteins indeed show the characteristics of signal peptides, that is, a positively charged N-terminal region followed by a central hydrophobic region of 7–12 residues and a more polar C-terminal region.

SDS PAGE showed that the intensity of the two bands corresponding to OmpA and OmpC was significantly lower than that of the capsid protein gp5, but was clearly higher than that of the portal protein gp3 (Figure 1B). This relative abundance of Sf6 structural proteins is in good agreement with that reported previously (Casjens et al., 2004). To further estimate the copy numbers of the two host proteins, we performed quantitation of the corresponding bands in Coomassie blue-stained SDS gels of the purified Sf6 virion (Table 3). It is well known that the portal protein and the tailspike protein are present in 12 and 18 copies respectively in many tailed dsDNA bacteriophages including the closely related P22 (Jiang et al., 2006; Johnson and Chiu, 2007; Lander et al., 2009; Lander et al., 2006; Tang et al., 2005). Thus, we chose to normalize the copy numbers against the gp3 portal protein, as in a previous study on SDS PAGE-based quantitation of protein copy numbers in phage T7 (Cerritelli et al., 2003). The quantitation showed approximately 36 and 32 copies of OmpA and OmpC respectively. As a control, the gp14 tailspike protein was present in 15 molecules in the virion as shown in the quantitation, which is close to the predicted 18 copies within the experimental error. This type of quantitation was not intended to determine the accurate molecular copy numbers. Nevertheless, it clearly indicates that approximately a few dozens of each of the two host OMPs are associated with the Sf6 virion.

CryoTEM structure of Sf6

We then analyzed the structure of Sf6 using cryoTEM to address how the two OMPs bound to the Sf6 virion. The icosahedrally averaged cryoTEM map of Sf6 shows a T=7*laevo* icosahedral capsid with an exterior morphology superimposable with the structure of closely related phage P22 (Jiang et al., 2003; Tang et al., 2006) (Figure 2A). However, extra density is clearly observed at quasi 3-fold, icosahedral 2-fold and icosahedral 3-fold axes at the interior surface of the capsid, which is not present in phage P22 (Figure 2D, E and F). The volume of these density can accommodate proteins of ~50kDa or ~460 amino acid residues in the icosahedral asymmetric unit, or 3MDa (27,600 residues) for the whole icosahedral capsid, when estimated using 1.3 mg/ml as the density for a protein. A difference map was calculated by subtracting the P22 capsid density from the Sf6 cryoTEM map, which shows major density located at the interior surface of the capsid (Figure 2F). Small islands of density are observed in this difference map at the outer surface of the capsid (Figure 2F), the largest of which can accommodate no more than 13 amino acid residues as estimated by their volumes, suggesting that they might be due to noise as structural difference of this scale in the Sf6 and P22 capsids may not be detectable at the current resolution.

The Sf6 capsid protein is similar to that of P22 in size (423 versus 430 residues), and the primary sequences of Sf6 and P22 capsid proteins show 14% identity and 45% similarity (Casjens et al., 2004). X-ray structures are available for HK97 matured capsid and procapsid (Gertsman et al., 2009; Wikoff et al., 2000), the minor capsid protein gp24 that forms pentameric vertices of the bacteriophage T4 capsid (Fokine et al., 2005), and putative capsid proteins of prophage (RCSB PDB codes 3BQW and 3BJQ). These and other previous structural data showed that the HK97 capsid protein represents a canonical fold shared by all tailed dsDNA bacteriophage as well as herpesvirus, even though their capsid proteins share low identity at the primary sequence level (Baker et al., 2005; Fokine et al., 2005; Jiang et al., 2008; Jiang et al., 2006; Jiang et al., 2003; Morais et al., 2005; Parent et al., 2010; Zhou et al., 2000). A search with the remote fold recognition tool PHYRE (Kelley and Sternberg, 2009) using the Sf6 capsid protein sequence identified the HK97 capsid protein structure as the top hit that has a fold similar to that of the N-terminal 280 residues of the Sf6 capsid

protein, although they share less than 10% sequence identity (Figure S2, supplementary data). The N-terminal portion of the P22 capsid protein also has the canonical HK97-like fold as revealed by cryoTEM, sequence analysis and structural modeling (Parent et al., 2010). Secondary structure prediction with PHYRE shows that the Sf6 and P22 capsid proteins both contain an N-terminal HK97-like domain and a C-terminal beta-strand-rich domain (Figure S2, supplementary data). Thus, the capsid proteins of Sf6 and P22 may share similar folds. This suggests that the major density revealed at the capsid inner surface in the difference map between Sf6 and P22 may arise from structural compositions other than the Sf6 capsid protein subunits.

We also fit the X-ray structure of HK97 capsid protein into the Sf6 cryoTEM map (Figure 2B and C). The optimal fitting was readily achieved without any rigid body movement of the HK97 structure, indicating structural similarity of the two phage capsids. The difference map between the Sf6 cryoTEM map and the fitted HK97 capsid protein structure showed two layers of density in the cryoTEM map that were not accounted for by the HK97 capsid protein structure (Figure 2B&C). The outer layer of density in the difference map might be due to the exterior surface protrusions of capsomers of the capsid (Figure 2C), which were also observed in P22 cryoTEM maps (Jiang et al., 2003; Parent et al., 2010) and were assigned as the C-terminal portions of P22 capsid proteins (Parent et al., 2010). This is consistent with the fact that the Sf6 and P22 capsid proteins are of similar size and are 141- and 148-residue longer than that of HK97, respectively. The inner layer of density in the difference map between the Sf6 cryoTEM map and the HK97 capsid model (colored in green in Figure 2C) is located at a low radius that corresponds to the inner surface of the capsid, and is virtually identical to the major density in the difference map between Sf6 and P22 (Figure 2F). As mentioned above, the volume of the major density located at the low radius can accommodate ~50kDa or ~460 amino acid residues in the icosahedral asymmetric unit if measured as proteins, therefore would unlikely be accounted for by any portions of Sf6 capsid protein that may adopt different structures than those of P22 or HK97. The consistent results of difference imaging suggest that the inner layer of density in both difference maps is likely due to the two host proteins associated with the Sf6 virion.

Fitting X-ray structural models of OmpA and OmpC into the Sf6 cryoTEM map

The inner layer of density revealed in the difference map is unlikely accounted for by the Sf6 capsid protein (Figure 2B&C), and was not present in phage P22 (Figure 2D). The density was located at four specific locations at the interior surface of the capsid with respect to the icosahedral lattice: near a quasi 3-fold axis surrounding the icosahedral 5-fold axis (Figure 3B), between a quasi 6-fold axis and a quasi 3-fold axis (Figure 3C), about the icosahedral 2-fold axis (Figure 3D), and about the icosahedral 3-fold axis (Figure 3E), which are designated as DQ3, DQ6, D2 and D3, respectively. The discernible unique shapes of these density allowed fitting available X-ray structures of highly homologous *E. coli* OmpA and OmpC into the Sf6 cryoTEM map. The elongated, nearly cylindrical density of DQ3, DQ6 and D2 fit well with the β-barrel structure of the OmpA transmembrane domain (Figure 3B, C and D) (Pautsch and Schulz, 2000). The D3 density at the icosahedral 3-fold axis showed an oblate cylindrical shape that fit well with the β-barrel structure of OmpC (Figure 3E) (Basle et al., 2006). Fitting of OmpC was evident also by an indentation of the density at the icosahedral 3-fold axis presumably owing to the inner pore of the β-barrel and the density that fit with the extracellular loop L2 of OmpC (Figure 3E; For nomenclature of loops in OmpC, see (Basle et al., 2006)). No strong density was present for other extracellular loops of fitted OmpC, which may be due to their conformational flexibility as evident by relatively high temperature factors in the X-ray structure and/or icosahedral symmetry averaging in cryoTEM reconstruction. Only a monomer of OmpA and OmpC was fitted into the density at the icosahedral 2-fold and 3-fold axis respectively, therefore, these

density reflected averaged images of bound OMPs, as icosahedral symmetry was imposed in the cryoEM reconstruction. In addition, the volumes of the density at the sites of DQ3, DQ6, D2 and D3 in the difference map corresponds to expected volumes for ~146, ~166, ~157 and ~207 amino acid residues respectively. These are in good agreement with sizes of the fitted OmpA and OmpC, which contain 137 and 180 residues for β-barrel regions respectively, considering the current resolution of the cryoTEM map.

Potential interactions of the fitted OMP structural models with the Sf6 capsid

While the current resolution of the Sf6 cryoTEM map prevents revelation of the atomic details of the OMP:capsid interactions, fitting of OMPs into the cryoTEM map provides a low-resolution picture regarding portions of OMPs and capsid protein subunits that participate in potential OMP:capsid interactions. This is based on the fitted OMP structural models and the pseudo-atomic model of the HK97 capsid structure fitted into the Sf6 cryoTEM map. The nomenclature for the HK97 capsid protein structure comprising A-domain, P-domain, E-loop and N-arm (Gertsman et al., 2009; Wikoff et al., 2000) (Figure 4A) is to be used in the following analysis. The fitted OmpC proteins are situated with the longitudinal axes of β-barrels perpendicular to the inner capsid surface (Figure 4). The periplasmic loops that connect β-strands in OmpC make direct contact with the P-domains of the fitted capsid protein models surrounding the icosahedral 3-fold axis, creating linkage among neighboring hexameric capsomers. OmpA lies nearly tangential to the inner capsid surface, and as a result, the OmpA molecules interact extensively with the capsid through the staves of their β-barrels and part of periplasmic and extracellular loops. The OmpA molecule at the DQ3 position lies against the P-domain of the capsid protein, where the majority of OmpA:capsid interactions occurs. This OmpA is close enough to the quasi 3-fold axis surrounding the icosahedral 5-fold axis such that the extracellular end of its β-barrel also interacts with the P-domain from capsid proteins in adjacent capsomers, bridging the neighboring pentameric and hexameric capsomers. The OmpA molecule at the DQ6 position makes contact mainly with the A-domain of the capsid protein, while its extracellular end interacts with the P-domain of the same capsid protein subunit. The OmpA molecule at the D2 position interacts with the P-domain and N-arms of the capsid proteins from neighboring hexameric capsomers, thus spanning icosahedral 2-fold axis-related hexameric capsomers. Thus, those OMPs create additional linkages among capsomers via non-covalent intermolecular interactions, which may contribute to the capsid stability.

DISCUSSION

We have identified two host-derived proteins, OmpA and OmpC, associated with the Sf6 virion using tandem mass spectrometry. CryoTEM and docking analysis provide evidence that the two proteins are likely located at specific sites at the interior surface of the phage capsid. The OmpC molecules are situated at the icosahedral 3-fold axes, while the OmpA molecules bind to three other sites in the icosahedral lattice. Assuming full occupancy, each Sf6 virion would contain 20 copies of OmpC and 150 copies of OmpA. However, the SDS gels did not show a significant excess of OmpA over OmpC (Figure 1B), and quantitation of the SDS gels showed that OmpA and OmpC were present in approximately 36 and 32 copies in the Sf6 virion respectively (Table 3). These suggest that OmpC may have nearly full occupancy whereas OmpA has a much lower occupancy. Such a difference in occupancy may arise from different binding affinity, different cellular supplies of the two OMPs, or shielding of binding sites by phage scaffolding proteins. While occupancy of the OmpA and OmpC binding sites varies, binding of the two proteins may create extra intermolecular interactions among capsomers, therefore may play a structural role akin to that of bacteriophage cementing proteins which stabilize the capsid to withstand the pressure resulted by highly dense packaging of phage DNA in the capsid (Smith et al., 2001).

Cementing proteins have been observed in several bacteriophage such as Soc and Hoc in T4 (Fokine et al., 2004), gpD in lambda (Yang et al., 2000), the Dec protein in L (Tang et al., 2006), the fiber in phi29 (Morais et al., 2005), the cementing protein in BPP-1 (Dai et al., 2010) and gp10 in epsilon15 (Jiang et al., 2008) as well as triplex proteins VP19c and VP23 in herpesvirus (Trus et al., 1996) and perhaps several minor capsid proteins in adenovirus (Rux and Burnett, 2004; Vellinga, Van der Heijdt, and Hoeben, 2005), which have been suggested to provide additional forces to stabilize the phage capsid. However, all these previously reported phage cementing proteins are phage-encoded and bind to the exterior surface of the phage capsid. Thus, association of OmpA and OmpC in Sf6 virion provides the first example of a bacteriophage that uses host-derived proteins as cementing materials, and they bind to the interior surface of the phage capsid.

The exteriorly-bound cementing proteins in these phages are thought to attach to the capsid in a later step in phage assembly, that is, after capsid maturation. Indeed, cementing proteins usually span neighboring capsid protein subunits, and their binding to the capsid requires proper relative positioning and orientation of capsid protein subunits. Drastic changes in inter-subunit positioning and orientation among neighboring capsid proteins during the procapsid-to-capsid maturation (Gertsman et al., 2009; Parent et al., 2010) ensures that the cementing protein-binding sites on the phage capsid are formed only in matured capsid but not in procapsid, therefore cementing protein binding occurs only after capsid maturation. However, in Sf6, the two host proteins are located at the interior of the virion. Thus, the OMPs must be pre-packed in the procapsid prior to maturation. This implies that two sets of structural determinants for OMP:Sf6 interactions are needed: one that targets the OMPs into the Sf6 procapsid, and the other that is responsible for OMP:capsid binding in the matured capsid as observed in the Sf6 cryoTEM structure.

The shapes of the density in the Sf6 cryoTEM map suggest that OmpA and OmpC associated with the Sf6 virion may be in folded forms. It is well known that bacterial OMPs are synthesized as unfolded polypeptides in cytoplasm, followed by translocation via the Sec translocon across plasma membrane into the periplasmic compartment, where they are processed by specific molecular chaperones into folded forms and inserted into the outer membrane (Bos, Robert, and Tommassen, 2007; Driessen and Nouwen, 2008; Knowles et al., 2009; Krojer et al., 2008; Rapoport, 2007; Ruiz, Kahne, and Silhavy, 2006). OmpA and OmpC possess an N-terminal signal sequence that directs them co- or post-translationally to the Sec translocon for translocation across the bacterial inner membrane (Bos, Robert, and Tommassen, 2007; Driessen and Nouwen, 2008; Rapoport, 2007; Ruiz, Kahne, and Silhavy, 2006). The signal sequence is cleaved upon OMP translocation across the bacterial inner membrane by a signal peptidase (Bernstein, 2000; Dalbey, 1991; Holland, 2004; Ruiz, Kahne, and Silhavy, 2006; von Heijne, 1990). Our N-terminal sequencing results showed that the signal sequences of both OMPs packed in the Sf6 virion were cleaved. Thus, it is likely that the two OMPs were subject to cleavage of signal sequences in the cytoplasm by an unknown mechanism, and were folded and packed into the Sf6 virion without being transported across the bacterial inner membrane. Cellular folding of OMPs occurs in the periplasmic compartment or at the bacterial outer membrane, which requires several molecular chaperones and folding machineries (Bos, Robert, and Tommassen, 2007; Knowles et al., 2009; Ruiz, Kahne, and Silhavy, 2006). These molecular chaperones and folding machineries are not available in the bacterial cytoplasm. While it can not be ruled out that the Sf6 procapsid may provide a molecular niche that assists folding of the two OMPs, it is more likely that some protein folding machinery located in the bacterial cytoplasm helps folding of the two packed OMPs. Additionally, this protein folding machinery may be spatially coupled with the phage assembly so that the newly folded OMPs are packed into the phage capsid in a timely manner. Thus, association of folded OmpA and OmpC with the Sf6 virion implies an alternative pathway for OMP folding

potentially using a chaperone located in the bacterial cytoplasm, and spatial coupling of phage assembly and the host protein folding machinery. A second possibility for trafficking of the two Sf6-packed OMPs is that they were transported into the periplasm as usual where the signal sequences were cleaved, and then traveled back into the cytoplasm to associate with the Sf6 viral proteins. This might be less favorable as it would require additional cellular machinery to transport the OMPs across the bacterial inner membrane in a direction opposite to the ordinary one.

Spatial coupling of cellular protein folding machineries and virus assembly have been recognized in studies of cellular sites termed virosome or viroplasm for eukaryotic virus replication and assembly (Netherton et al., 2007; Novoa et al., 2005). It's not known if similar sites in prokaryotic host cells are used for bacteriophage replication and assembly. An example of connection between cellular protein folding mechanism and bacteriophage replication is for T4, which encodes a GroES-like protein gp31 that can interact with the host chaperone GroEL to aid phage protein folding (Clare et al., 2009; van der Vies, Gatenby, and Georgopoulos, 1994). Nevertheless, such a phage-encoded protein doesn't seem to be present in Sf6 based on open reading frames predicted from the genomic sequence (Casjens et al., 2004). Our finding that Sf6 virion packs two host outer membrane proteins reveals a new linkage between bacteriophage assembly and host protein-folding mechanisms that is akin to eukaryotic viruses.

It is interesting to point out that genomes of a few lambdoid bacteriophage contain OmpC-like genes that were thought to be expressed to make phage-encoded porins during the lysogenic state, and these phage used the host OmpC as their cellular receptors (Blasband, Marcotte, and Schnaitman, 1986; Highton et al., 1985). It was speculated that expression of the phage-encoded porin strongly inhibited expression of the host porin, and when such a lysogen was induced, there would be little host-encoded porin on the cell surface to neutralize progeny phage, which was advantageous to the phage (Blasband, Marcotte, and Schnaitman, 1986). However, the Sf6 genome doesn't seem to contain any OMP-like gene (Casjens et al., 2004), and the cellular receptor of Sf6 is not known. On the other hand, OmpC is involved in invasion of epithelial cells by *S. flexneri* (Bernardini et al., 1993). Alteration of OMPs has been shown to contribute to drug-resistance in Gram-negative bacteria (Pages, James, and Winterhalter, 2008; Raja, Murali, and Devaraj, 2008). Nevertheless, the implication of the OMP presence in the Sf6 virion on Sf6:Shigella interaction is perplexing. Further studies are needed to address a series of questions such as how the OMPs bind to the Sf6 capsid inner surface in detail, if and how those packed OMPs affects the Sf6 lifecycle and/or the infected host cells, what cytoplasmic chaperone is involved in folding of the OMPs to be packed in Sf6, and how this membrane protein folding machinery is coupled with phage assembly.

MATERIALS AND METHODS

Virus purification

The Sf6 strain was a gift from Dr. S.C. Casjens at the University of Utah and was described (Casjens et al., 2004). The Sf6 virion was propagated in *Shigella flexneri* strain M94 and was carefully purified using cesium gradient ultracentrifugation as following. A single colony of S. flexneri was used to inoculate a 10ml LB broth and grow overnight at 37°C. The 150ml fresh LB broth was inoculated with 10 ml overnight culture and grown to OD600 close to 1.0. At this point, 100μl Sf6 virion was added to the LB culture, shaken at 37°C and measured OD600 every hour untill OD600 decreased to 0.2 which indicated that partial lysis occurred. The culture was then shaken with chloroform to complete lysis for another hour, the cell debris was removed by centrifugation with a Sorvall GSA rotor for 20 minutes at 8,000 rpm. The sf6 virion was pelleted for 18 hours at 8,000 rpm in the GSA rotor. The

pellet was resuspended slowly by gentle pipetting in 5ml TM buffer (10mM Tris-HCl pH7.4, 1mM MgCl2) at 4°C for 2 hours, and the solution was milky with some aggregated material, which was removed by centrifugation for 15 minutes at 4,000 rpm (Eppendorf 5810R). The supernatant was carefully applied on the top of a CsCl step gradient which contained 2ml 20% sucrose solution on the top, 2ml 1.4g/ml CsCl solution in the middle, and 2ml 1.6g/ml CsCl solution at the bottom (all solutions were made with the TM buffer). This was spun for 2 hours in a Beckman SW40 rotor at 25,000 rpm at 4°C. A sharp opalescent virion band was readily observed at the boundary between the 1.4 and 1.6 g/ml CsCl solutions, and was harvested by syringe puncture from the side of the centrifuge tube followed by dialysis against the TM buffer. This preparation was subject to a second run of CsCl gradient ultracentrifugation in order to thoroughly remove residual contaminants. The purified virus preparation was of high homogeneity and free of membranous debris as confirmed by negative staining electron microscopy (Figure 1A). The purified Sf6 virions were concentrated with Amicon Ultra-4 (100,000 MWCO) for subsequent SDS-PAGE and cryoTEM analysis.

SDS gel quantitation and protein N-terminal sequencing

The purified Sf6 virion was subjected to SDS PAGE. The Coomassie blue-stained gels were imaged on an AlphaImager EP gel documentation system, and the gel images were quantitated with the AlphaView image analysis software provided by the manufacturer. Four batches of purified Sf6 virion were subject to quantitation, yielding four measurements, where the average copy numbers of proteins were obtained.

For N-terminal protein sequencing, the purified Sf6 virion was subject to SDS PAGE. The proteins were transferred from the gel to the PVDF membrane, followed by Coomassie blue staining. The two bands corresponding to OmpA and OmpC were excised from the PVDF membrane, washed for 6 times with deionized water, and loaded onto a Model 494 Procise protein/peptide sequencer with an on-line Model 140C PTH Amino Acid Analyzer (Applied Biosystems, Inc.) at the Iowa State University Protein Facility for sequence analysis.

Protein identification by tandem mass spectrometry

The purified Sf6 virion was subjected to SDS PAGE. The bands corresponding to the two previously unidentified proteins were excised from the gel, digested with trypsin, and subjected to capillary LC-MS/MS experiments using tandem LTQ-FT Mass Spectrometer (ThermoFinnigan) as described (Ikehata et al., 2008). MS/MS peak lists were created in the dta format from XCalibur raw files using the Bioworks (Thermo, version 2.0) software. Mascot (Matrix Science, version 2.2) and X!Tandem (www.thegpm.org) algorithms were used to perform MS/MS database search against the NCBInr_20081206 database (7463447 entries) with a fragment ion mass tolerance of 0.20 Da and a parent ion tolerance of 10.0 PPM. Iodoacetamide derivative of cysteine was specified as a fixed modification. The Scaffold software (Proteome Software Inc., version 2.06) was used to combine and validate MS/MS based peptide and protein identifications. Besides Omp proteins, only trypsin and keratin were identified at greater than 20.0% probability that were assigned by the Protein Prophet algorithm (Nesvizhskii et al., 2003). Peptide identifications with greater than 50.0% probability as specified by the Peptide Prophet algorithm (Keller et al., 2002) were accepted for reporting protein coverage.

CryoTEM and image reconstruction

The purified virus was frozen-hydrated in vitrified ice on holey EM grids, and subject to cryoTEM by standard procedures (Adrian et al., 1984; van Heel et al., 2000) on an FEI Tecnai F20 G2 transmission electron microscope equipped with field emission gun operated at an accelerating voltage of 200kV. Electron micrographs were recorded under a dose of

~20 electrons per $Å^2$ with defocus values in the range of −0.47 to −1.06 microns and a magnification of 39,000. A total of 3,232 particle images were boxed from 79 electron micrographs in a dimension of 200×200 with a pixel size of 4.05 Å/pixel. The three-dimensional reconstruction was calculated and refined with the program SPIDER (Frank et al., 1996), using the cryoTEM map of P22 as the initial model (Tang et al., 2006). The resolution of the reconstruction was 19Å as estimated with the program RMEASURE (Sousa and Grigorieff, 2007). The contrast transfer function (CTF) correction was not performed, as the resolution limit of the final reconstruction was within the first zero of the CTFs. The cryoEM maps shown in Figures 2A, B and D and Figure 3A were contoured at 1.31 sigma above the background. This contour level is selected so that the resulting volume represents the expected volume of the capsid proteins and the OmpA/OmpC proteins. At this contour level, no density was observed inside the phage capsid that can be putatively assigned to the packaged DNA.

Difference map and fitting of molecular structures

The cryoTEM map of Sf6 was superimposed with that of the evolutionarily and structurally related phage P22 (Tang et al., 2006). Extra density in the Sf6 map that was not present in the P22 cryoEM map was readily observed at the inner surface of the capsid. The Sf6 and P22 maps were normalized, and a difference map was calculated by subtracting the P22 map from the Sf6 map. The X-ray structure of HK97 mature capsid (RCSB PDB entry 1ohg) was fitted into the Sf6 cryoTEM map without re-orientation or re-positioning of the capsid proteins, but the optimal fitting was achieved with 3% shrinkage of the Sf6 cryoTEM map, which is within the range of experimental error of the nominal magnification of the electron microscope. A difference map was calculated by subtracting the density of the fitted HK97 capsid model from the Sf6 cryoTEM map. The OmpA and OmpC X-ray structures (Basle et al., 2006; Pautsch and Schulz, 2000) were manually fitted into the difference map with the program O (Jones et al., 1991) and optimized with the “Fit in Map” function of UCSF Chimera (Goddard, Huang, and Ferrin, 2007). The distinct shapes of the density, either elongated cylindrical or oblate cylindrical, allowed distinguishing between OmpA and OmpC. There was no steric clash for polypeptide main chains between the fitted OmpA and OmpC models and the capsid model derived from the fitted HK97 structure.

Accession codes

The cryoTEM map of Sf6 and the fitted OMP coordinates have been deposited with the European Bioinformatics Institute Electron Microscopy Data Bank under the accession code EMD-5201 and RCSB Protein Data Bank under the accession code 3NB3, respectively.

Supplementary Material

Refer to Web version on PubMed Central for supplementary material.

Acknowledgments

We thank Dr. Sherwood Casjens at the University of Utah for kindly sharing the bacteriophage Sf6 strain. This work was supported by the NIH grant R01GM090010 to L.T.

References

Adrian M, Dubochet J, Lepault J, McDowall AW. Cryo-electron microscopy of viruses. Nature 1984;308(5954):32–6. [PubMed: 6322001]

Baker ML, Jiang W, Rixon FJ, Chiu W. Common ancestry of herpesviruses and tailed DNA bacteriophages. J Virol 2005;79(23):14967–70. [PubMed: 16282496]

Basle A, Rummel G, Storici P, Rosenbusch JP, Schirmer T. Crystal structure of osmoporin OmpC from E. coli at 2.0 A. J Mol Biol 2006;362(5):933–42. [PubMed: 16949612]

Bechtel JT, Winant RC, Ganem D. Host and viral proteins in the virion of Kaposi's sarcoma-associated herpesvirus. J Virol 2005;79(8):4952–64. [PubMed: 15795281]

Bendtsen JD, Nielsen H, von Heijne G, Brunak S. Improved prediction of signal peptides: SignalP 3.0. J Mol Biol 2004;340(4):783–95. [PubMed: 15223320]

Bernardini ML, Sanna MG, Fontaine A, Sansonetti PJ. OmpC is involved in invasion of epithelial cells by Shigella flexneri. Infect Immun 1993;61(9):3625–35. [PubMed: 8359885]

Bernstein HD. The biogenesis and assembly of bacterial membrane proteins. Curr Opin Microbiol 2000;3(2):203–9. [PubMed: 10744997]

Blasband AJ, Marcotte WR Jr, Schnaitman CA. Structure of the lc and nmpC outer membrane porin protein genes of lambdoid bacteriophage. J Biol Chem 1986;261(27):12723–32. [PubMed: 3017988]

Bos MP, Robert V, Tommassen J. Biogenesis of the gram-negative bacterial outer membrane. Annu Rev Microbiol 2007;61:191–214. [PubMed: 17506684]

Casjens S, Winn-Stapley DA, Gilcrease EB, Morona R, Kuhlewein C, Chua JE, Manning PA, Inwood W, Clark AJ. The chromosome of Shigella flexneri bacteriophage Sf6: complete nucleotide sequence, genetic mosaicism, and DNA packaging. J Mol Biol 2004;339(2):379–94. [PubMed: 15136040]

Cerritelli ME, Trus BL, Smith CS, Cheng N, Conway JF, Steven AC. A second symmetry mismatch at the portal vertex of bacteriophage T7: 8-fold symmetry in the procapsid core. J Mol Biol 2003;327(1):1–6. [PubMed: 12614603]

Clare DK, Bakkes PJ, van Heerikhuizen H, van der Vies SM, Saibil HR. Chaperonin complex with a newly folded protein encapsulated in the folding chamber. Nature 2009;457(7225):107–10. [PubMed: 19122642]

Dai W, Hodes A, Hui WH, Gingery M, Miller JF, Zhou ZH. Three-dimensional structure of tropism-switching Bordetella bacteriophage. Proc Natl Acad Sci U S A 2010;107(9):4347–52. [PubMed: 20160083]

Dalbey RE. Leader peptidase. Mol Microbiol 1991;5(12):2855–60. [PubMed: 1809829]

de Beer T, Fang J, Ortega M, Yang Q, Maes L, Duffy C, Berton N, Sippy J, Overduin M, Feiss M, Catalano CE. Insights into specific DNA recognition during the assembly of a viral genome packaging machine. Mol Cell 2002;9(5):981–91. [PubMed: 12049735]

Dokland T. Scaffolding proteins and their role in virus assembly. Cell Mol Life Sci 1999;56:580–603. [PubMed: 11212308]

Driessen AJ, Nouwen N. Protein translocation across the bacterial cytoplasmic membrane. Annu Rev Biochem 2008;77:643–67. [PubMed: 18078384]

Fane BA, Prevelige PE Jr. Mechanism of scaffolding-assisted viral assembly. Adv Protein Chem 2003;64:259–99. [PubMed: 13677050]

Fanning E, Zhao K. SV40 DNA replication: from the A gene to a nanomachine. Virology 2009;384(2): 352–9. [PubMed: 19101707]

Fokine A, Chipman PR, Leiman PG, Mesyanzhinov VV, Rao VB, Rossmann MG. Molecular architecture of the prolate head of bacteriophage T4. Proc Natl Acad Sci U S A 2004;101(16): 6003–8. [PubMed: 15071181]

Fokine A, Leiman PG, Shneider MM, Ahvazi B, Boeshans KM, Steven AC, Black LW, Mesyanzhinov VV, Rossmann MG. Structural and functional similarities between the capsid proteins of bacteriophages T4 and HK97 point to a common ancestry. Proc Natl Acad Sci U S A 2005;102(20):7163–8. [PubMed: 15878991]

Frank J, Radermacher M, Penczek P, Zhu J, Li Y, Ladjadj M, Leith A. SPIDER and WEB: processing and visualization of images in 3D electron microscopy and related fields. J Struct Biol 1996;116(1):190–9. [PubMed: 8742743]

Franke EK, Yuan HE, Luban J. Specific incorporation of cyclophilin A into HIV-1 virions. Nature 1994;372(6504):359–62. [PubMed: 7969494]

Gemski P Jr, Koeltzow DE, Formal SB. Phage conversion of Shigella flexneri group antigens. Infect Immun 1975;11(4):685–91. [PubMed: 1091548]

Gertsman I, Gan L, Guttman M, Lee K, Speir JA, Duda RL, Hendrix RW, Komives EA, Johnson JE. An unexpected twist in viral capsid maturation. Nature 2009;458(7238):646–50. [PubMed: 19204733]

Goddard TD, Huang CC, Ferrin TE. Visualizing density maps with UCSF Chimera. J Struct Biol 2007;157(1):281–7. [PubMed: 16963278]

Highton PJ, Chang Y, Marcotte WR Jr, Schnaitman CA. Evidence that the outer membrane protein gene nmpC of Escherichia coli K-12 lies within the defective qsr' prophage. J Bacteriol 1985;162(1):256–62. [PubMed: 2984173]

Holland IB. Translocation of bacterial proteins--an overview. Biochim Biophys Acta 2004;1694(1–3): 5–16. [PubMed: 15546654]

Homa FL, Brown JC. Capsid assembly and DNA packaging in herpes simplex virus. Rev Med Virol 1997;7(2):107–122. [PubMed: 10398476]

Ikehata K, Duzhak TG, Galeva NA, Ji T, Koen YM, Hanzlik RP. Protein targets of reactive metabolites of thiobenzamide in rat liver in vivo. Chem Res Toxicol 2008;21(7):1432–42. [PubMed: 18547066]

Ishidate K, Creeger ES, Zrike J, Deb S, Glauner B, MacAlister TJ, Rothfield LI. Isolation of differentiated membrane domains from Escherichia coli and Salmonella typhimurium, including a fraction containing attachment sites between the inner and outer membranes and the murein skeleton of the cell envelope. J Biol Chem 1986;261(1):428–43. [PubMed: 3510202]

Jiang W, Baker ML, Jakana J, Weigele PR, King J, Chiu W. Backbone structure of the infectious epsilon15 virus capsid revealed by electron cryomicroscopy. Nature 2008;451(7182):1130–4. [PubMed: 18305544]

Jiang W, Chang J, Jakana J, Weigele P, King J, Chiu W. Structure of epsilon15 bacteriophage reveals genome organization and DNA packaging/injection apparatus. Nature 2006;439(7076):612–6. [PubMed: 16452981]

Jiang W, Li Z, Zhang Z, Baker ML, Prevelige PE Jr, Chiu W. Coat protein fold and maturation transition of bacteriophage P22 seen at subnanometer resolutions. Nat Struct Biol 2003;10(2):131–5. [PubMed: 12536205]

Johnson JE. Virus particle maturation: insights into elegantly programmed nanomachines. Curr Opin Struct Biol 2010;20(2):210–6. [PubMed: 20149636]

Johnson JE, Chiu W. DNA packaging and delivery machines in tailed bacteriophages. Curr Opin Struct Biol 2007;17(2):237–43. [PubMed: 17395453]

Jones TA, Zou JY, Cowan SW, Kjeldgaard M. Improved methods for building protein models in electron density maps and the location of errors in these models. Acta Crystallogr A 1991;47 (Pt 2):110–9. [PubMed: 2025413]

Keller A, Nesvizhskii AI, Kolker E, Aebersold R. Empirical statistical model to estimate the accuracy of peptide identifications made by MS/MS and database search. Anal Chem 2002;74(20):5383–92. [PubMed: 12403597]

Kelley LA, Sternberg MJ. Protein structure prediction on the Web: a case study using the Phyre server. Nat Protoc 2009;4(3):363–71. [PubMed: 19247286]

Knowles TJ, Scott-Tucker A, Overduin M, Henderson IR. Membrane protein architects: the role of the BAM complex in outer membrane protein assembly. Nat Rev Microbiol 2009;7(3):206–14. [PubMed: 19182809]

Krojer T, Sawa J, Schafer E, Saibil HR, Ehrmann M, Clausen T. Structural basis for the regulated protease and chaperone function of DegP. Nature 2008;453(7197):885–90. [PubMed: 18496527]

Lander GC, Khayat R, Li R, Prevelige PE, Potter CS, Carragher B, Johnson JE. The P22 tail machine at subnanometer resolution reveals the architecture of an infection conduit. Structure 2009;17(6): 789–99. [PubMed: 19523897]

Lander GC, Tang L, Casjens SR, Gilcrease EB, Prevelige P, Poliakov A, Potter CS, Carragher B, Johnson JE. The structure of an infectious P22 virion shows the signal for headful DNA packaging. Science 2006;312(5781):1791–5. [PubMed: 16709746]

Lindberg AA, Wollin R, Gemski P, Wohlhieter JA. Interaction between bacteriophage Sf6 and Shigella flexner. J Virol 1978;27(1):38–44. [PubMed: 357756]

Loret S, Guay G, Lippe R. Comprehensive characterization of extracellular herpes simplex virus type 1 virions. J Virol 2008;82(17):8605–18. [PubMed: 18596102]

Morais MC, Choi KH, Koti JS, Chipman PR, Anderson DL, Rossmann MG. Conservation of the capsid structure in tailed dsDNA bacteriophages: the pseudoatomic structure of phi29. Mol Cell 2005;18(2):149–59. [PubMed: 15837419]

Nesvizhskii AI, Keller A, Kolker E, Aebersold R. A statistical model for identifying proteins by tandem mass spectrometry. Anal Chem 2003;75(17):4646–58. [PubMed: 14632076]

Netherton C, Moffat K, Brooks E, Wileman T. A guide to viral inclusions, membrane rearrangements, factories, and viroplasm produced during virus replication. Adv Virus Res 2007;70:101–82. [PubMed: 17765705]

Novoa RR, Calderita G, Arranz R, Fontana J, Granzow H, Risco C. Virus factories: associations of cell organelles for viral replication and morphogenesis. Biol Cell 2005;97(2):147–72. [PubMed: 15656780]

Pages JM, James CE, Winterhalter M. The porin and the permeating antibiotic: a selective diffusion barrier in Gram-negative bacteria. Nat Rev Microbiol 2008;6(12):893–903. [PubMed: 18997824]

Parent KN, Khayat R, Tu LH, Suhanovsky MM, Cortines JR, Teschke CM, Johnson JE, Baker TS. P22 coat protein structures reveal a novel mechanism for capsid maturation: stability without auxiliary proteins or chemical crosslinks. Structure 2010;18(3):390–401. [PubMed: 20223221]

Pautsch A, Schulz GE. High-resolution structure of the OmpA membrane domain. J Mol Biol 2000;298(2):273–82. [PubMed: 10764596]

Raja SB, Murali MR, Devaraj SN. Differential expression of ompC and ompF in multidrug-resistant Shigella dysenteriae and Shigella flexneri by aqueous extract of Aegle marmelos, altering its susceptibility toward beta-lactam antibiotics. Diagn Microbiol Infect Dis 2008;61(3):321–8. [PubMed: 18358664]

Rao VB, Feiss M. The bacteriophage DNA packaging motor. Annu Rev Genet 2008;42:647–81. [PubMed: 18687036]

Rapoport TA. Protein translocation across the eukaryotic endoplasmic reticulum and bacterial plasma membranes. Nature 2007;450(7170):663–9. [PubMed: 18046402]

Ruiz N, Kahne D, Silhavy TJ. Advances in understanding bacterial outer-membrane biogenesis. Nat Rev Microbiol 2006;4(1):57–66. [PubMed: 16357861]

Rux JJ, Burnett RM. Adenovirus structure. Hum Gene Ther 2004;15(12):1167–76. [PubMed: 15684694]

Smith DE, Tans SJ, Smith SB, Grimes S, Anderson DL, Bustamante C. The bacteriophage straight phi29 portal motor can package DNA against a large internal force. Nature 2001;413(6857):748–52. [PubMed: 11607035]

Sousa D, Grigorieff N. Ab initio resolution measurement for single particle structures. J Struct Biol 2007;157(1):201–10. [PubMed: 17029845]

Steven AC, Heymann JB, Cheng N, Trus BL, Conway JF. Virus maturation: dynamics and mechanism of a stabilizing structural transition that leads to infectivity. Curr Opin Struct Biol 2005;15(2):227–36. [PubMed: 15837183]

Tang L, Gilcrease EB, Casjens SR, Johnson JE. Highly discriminatory binding of capsid-cementing proteins in bacteriophage L. Structure 2006;14(5):837–45. [PubMed: 16698545]

Tang L, Marion WR, Cingolani G, Prevelige PE, Johnson JE. Three-dimensional structure of the bacteriophage P22 tail machine. Embo J 2005;24(12):2087–95. [PubMed: 15933718]

Trus BL, Booy FP, Newcomb WW, Brown JC, Homa FL, Thomsen DR, Steven AC. The herpes simplex virus procapsid: structure, conformational changes upon maturation, and roles of the triplex proteins VP19c and VP23 in assembly. J Mol Biol 1996;263(3):447–62. [PubMed: 8918600]

van der Vies SM, Gatenby AA, Georgopoulos C. Bacteriophage T4 encodes a co-chaperonin that can substitute for Escherichia coli GroES in protein folding. Nature 1994;368(6472):654–6. [PubMed: 7908418]

van Heel M, Gowen B, Matadeen R, Orlova EV, Finn R, Pape T, Cohen D, Stark H, Schmidt R, Schatz M, Patwardhan A. Single-particle electron cryo-microscopy: towards atomic resolution. Q Rev Biophys 2000;33(4):307–69. [PubMed: 11233408]

Vellinga J, Van der Heijdt S, Hoeben RC. The adenovirus capsid: major progress in minor proteins. J Gen Virol 2005;86(Pt 6):1581–8. [PubMed: 15914835]

von Heijne G. The signal peptide. J Membr Biol 1990;115(3):195–201. [PubMed: 2197415]

Wikoff WR, Liljas L, Duda RL, Tsuruta H, Hendrix RW, Johnson JE. Topologically linked protein rings in the bacteriophage HK97 capsid. Science 2000;289(5487):2129–33. [PubMed: 11000116]

Xin W, Feiss M. Function of IHF in lambda DNA packaging. I. Identification of the strong binding site for integration host factor and the locus for intrinsic bending in cosB. J Mol Biol 1993;230(2): 492–504. [PubMed: 8385227]

Yang F, Forrer P, Dauter Z, Conway JF, Cheng N, Cerritelli ME, Steven AC, Pluckthun A, Wlodawer A. Novel fold and capsid-binding properties of the lambda-phage display platform protein gpD. Nat Struct Biol 2000;7(3):230–7. [PubMed: 10700283]

Zhou ZH, Dougherty M, Jakana J, He J, Rixon FJ, Chiu W. Seeing the herpesvirus capsid at 8.5 A. Science 2000;288(5467):877–80. [PubMed: 10797014]

Zhu FX, Chong JM, Wu L, Yuan Y. Virion proteins of Kaposi's sarcoma-associated herpesvirus. J Virol 2005;79(2):800–11. [PubMed: 15613308]

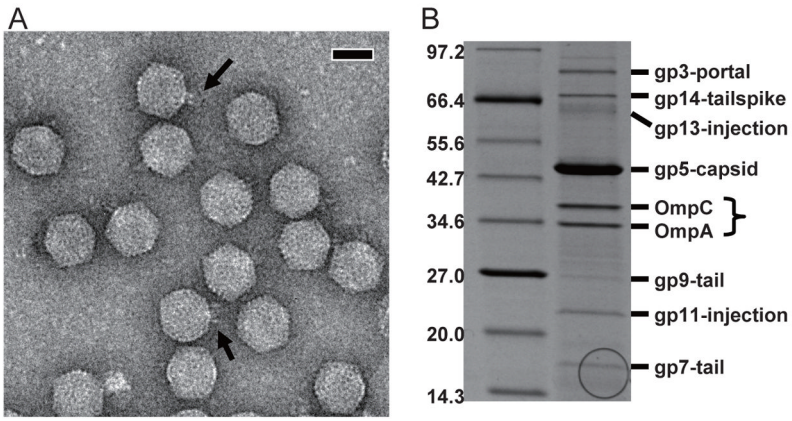

Figure 1. Characterization proteins present in the Sf6 virion

(A) Electron micrograph of the purified Sf6 virions negatively stained with 1% uranyl acetate. Tails of some virus particles are clearly visible (arrows). Bar, ~500 Å.

(B) SDS-PAGE of the purified Sf6 virions (right lane). Left lane, MW marker shown in kDa (Invitrogen). Phage-encoded structural proteins of the Sf6 virion are labeled. The two bands that were identified as OmpA and OmpC with mass spectrometry are indicated.

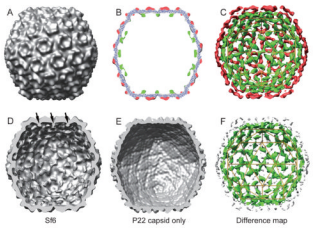

Figure 2. CryoTEM structure of the Sf6 virion

(A) The cryoTEM map of the Sf6 virion contoured at 1.31 sigma above the background viewed down an icosahedral 2-fold axis.

(B) A 20Å-thick central section of Sf6 cryoTEM map superimposed with fitted HK97 capsid structure (Cα trace in blue). The part of the map that is accounted for by the docked HK97 structure is in grey. The interior and exterior density that is not accounted for by the fitted HK97 structure is in green and red, respectively.

(C) The difference map derived by subtracting the fitted HK97 structure from the Sf6 cryoTEM map. An icosahedral lattice (yellow sticks) is superimposed to show locations of icosahedral and quasi symmetric axes. In C, D, E and F, the front half was computationally removed for visualization of internal features.

(D) Cut-away view of the Sf6 cryoTEM map showing significant density (arrows) that is not present in P22 in panel (E). Notice these density is located at the interior surface of Sf6 capsid, and is in sharp contrast to the relatively smooth interior surface of P22 capsid in (E).

(E) Cut-away view of the P22 cryoTEM map, in which only the capsid portion is shown and the DNA density was removed computationally, enabled by a ~20 Å gap between the capsid and the DNA density (Figure S1, supplementary data).

(F) Cut-away view of the difference map between Sf6 and the P22 capsid superimposed with the icosahedral lattice (yellow). Notice the major density in this difference map colored green is virtually identical to the density (green) at the capsid inner surface in the difference map in (C). Small islands of density at the higher radius of the capsid (grey) may be due to noise.

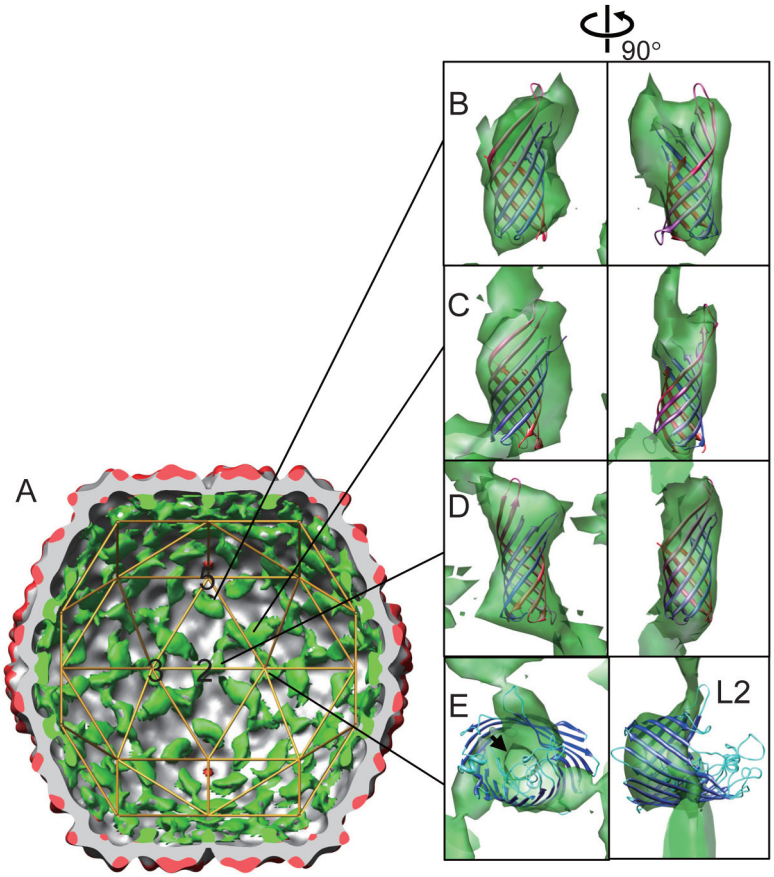

Figure 3. Fitting of OmpA and OmpC into the Sf6 cryoTEM map

(A) CryoTEM map of the Sf6 virion superimposed with the icosahedral lattice (yellow sticks). The color scheme is the same as in Figure 2B. The icosahedral two-, three-, and five-fold axes are indicated with 2, 3 and 5, respectively.

(B–E) Fitting of X-ray structures of OmpA (B, C and D) and OmpC (E) into the difference map (semi-transparent surface in green). In each pan from the left one about the vertical axis. The X-ray structures are shown as ribbon diagrams ramp-colored from blue (N-terminus) to red (C-terminus) for OmpA, and in blue for the β-barrel and in cyan for loops for OmpC. In (E), the indentation of the density putatively due to the pore of OmpC is indicated with an arrow, and the OmpC extracellular loop L2 is labeled.

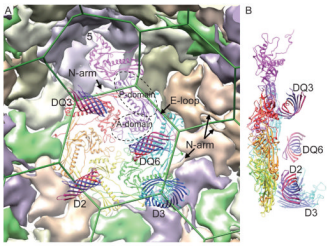

Figure 4. Interactions of OmpA and OmpC with the capsid

(A) Superimposition of the fitted OmpA and OmpC with the capsid model derived from the HK97 X-ray structure. The capsid model in the icosahedral asymmetric unit and associated OmpA (labeled with DQ3, DQ6 and D2) and OmpC (labeled with D3) are shown as ribbon diagrams. Neighboring capsid protein subunits are shown as molecular surface. The color scheme for OmpA and OmpC is the same as in Figure 3. The seven capsid protein subunits are colored differently, one of which is labeled with A-domain, P-domain, E-loop and N-arm according to the convention in the HK97 structure. An icosahedral five-fold vertex is indicated with 5. The hexagonal lattice of the icosahedral capsid is shown as sticks in green. The view is approximately down the quasi 6-fold axis.

(B) The view in (A) is rotated by 90° about the vertical axis. Only the capsid model in the icosahedral asymmetric unit and associated OmpA and OmpC are shown.

Table 1

Unique peptides identified for the two non-virally encoded proteins

Matched protein	NCBI accession number	Size of the matched protein	Sequence coverage	Mascot search score	Unique peptides identified (Start and end residue numbers and sequences are shown. The residues immediately before and after each cleavage site are also shown and are separated from the identified peptide by a dot.)
OmpC	gi|24113600	41,377 Da (373 aa)	52%	770	38–48 K.VDGLHYFSDDK.S 103–113 K.FQDVGSFDYGR.N 154–173 R.STDFFGLVDGLNFAVQYQGK.N 192–218 R.QNGDGVGGSITYDYEGFGIGAAVSSSK.R 219–229 K.RTDDQNFGLNR.Y 220–229 R.TDDQNFGLNR.Y 241–249 R.AETYTGGLK.Y 250–269 K.YDANNIYLAAQYTQTYNATR.V 270–278 R.VGNLGWANK.A 279–304 K.AQNFEAVAQYQFDFGLRPSLAYLQSK.G 315–323 R.NYDDEDILK.Y 324–335 K.YVDVGATYYFNK.N 345–355 K.INLLDDNQFTR.D 356–373 R.DAGINTDNIVALGLVYQF.-
OmpA	gi|30062494	37,374 Da (348 aa)	47%	736	104–117 K.LGYPITDDLDIYTR.L 129–138 K.ANVPGGASFK.D 139–163 K.DHDTGVSPVFAGGVEYAITPEIATR.L 195–215 R.FGQGEAAPVVAPAPAPEVQTK.H 221–229 K.SDVLFNFNK.A 230–253 K.ATLKPEGQAALDQLYSQLSNLDPK.D 254–265 K.DGSVVVLGYTDR.I 266–278 R.IGSDAYNQGLSER.R 279–290 R.RAQSVVDYLISK.G 280–290 R.AQSVVDYLISK.G 320–330 R.AALIDCLAPDR.R 338–348 K.GIKDVVTQPQA.-

Table 2

Primary sequences of OmpC and OmpA. The matched peptides in mass spectrometry are in bold and underlined. Residue numbers are shown for every 50 residues.

OmpC	**1**	MKVKVLSLLV	PALLVAGAAN	AAEVYNKDGN	KLDLYGK**VDG**	**LHYFSDDK**SV
	51	DGDQTYMRLG	FKGETQVTDQ	LTGYGQWEYQ	IQGNSAENEN	NSWTRVAFAG
	101	LK**FQDVGSFD**	**YGR**NYGVVYD	VTSWTDVLPE	FGGDTYGSDN	FMQQRGNGFA
	151	TYR**STDFFGL**	**VDGLNFAVQY**	**QGK**NGSPEGE	GMTNNGREAL	R**QNGDGVGGS**
	201	**ITYDYEGFGI**	**GAAVSSSKRT**	**DDQNFGLNR**Y	DERYIGNGDR	**AETYTGGLKY**
	251	**DANNIYLAAQ**	**YTQTYNATRV**	**GNLGWANKAQ**	**NFEAVAQYQF**	**DFGLRPSLAY**
	301	**LQSK**GKNLGV	INGR**NYDDED**	**ILKYVDVGAT**	**YYFNK**NMSTY	VDYK**INLLDD**
	351	**NQFTRDAGIN**	**TDNIVALGLV**	**YQF**		
OmpA	**1**	MKKTAIAIAV	ALAGFATVAQ	AAPKDNTWYT	GAKLGWSQYH	DTGFIPNNGP
	51	THENQLGAGA	FGGYQVNPYV	GFEMGYDWLG	RMPYKGDNIN	GAYKAQGVQL
	101	TAK**LGYPITD**	**DLDIYTR**LGG	MVWRADTK**AN**	**VPGGASFKDH**	**DTGVSPVFAG**
	151	**GVEYAITPEI**	**ATR**LEYQWTN	NIGDANTIGT	RPDNGLLSLG	VSYR**FGQGEA**
	201	**APVVAPAPAP**	**EVQTK**HFTLK	**SDVLFNFNKA**	**TLKPEGQAAL**	**DQLYSQLSNL**
	251	**DPKDGSVVVL**	**GYTDRIGSDA**	**YNQGLSERRA**	**QSVVDYLISK**	GIPADKISAR
	301	GMGESNPVTG	NTCDNVKQR**A**	**ALIDCLAPDR**	RVEIEVK**GIK**	**DVVTQPQA**

Table 3

Quantitation of proteins in the purified Sf6 virion.

Protein	MW/Da	Average copy number in a virion*	Standard deviation*
gp3 (portal)	79,469	(12)	-
gp14 (tailspike)	67,066	15.1	1.6
OmpC	41,377	31.7	6.5
OmpA	37,374	36.2	5.6

*Number of measurements: 4.